DOI: 10.13009/EUCASS2019-81



# Planetary Exploration of Saturn moons Dione and Enceladus

***Juan R. Sanmartín* and J. Peláez*****

* *Real Academia de Ingeniería*
*Universidad Politécnica de Madrid*
*Pza. C. Cisneros 3*, Madrid 28040, *juan.r.sanmartin@upm.es*

** *Universidad Politécnica de Madrid*
*Pza. C. Cisneros 3*, Madrid 28040, *j.pelaez@upm.es*

## Abstract

Search for habitability in *Outer* planets moons, requires presence of water, energy, and proper chemistry. Dissipation from tidal forces is major energy source in evolution of *Icy moon* systems. Saturn moons *Enceladus* and *Dione* are in 1:2 *Laplace* resonance. Enceladus ejects plumes of water vapor and ice particles, Dione exhibits *linear virgae*, hundred kilometres long, *latitudinal* color lines. A minor tether mission would explore this system. Following Saturn capture, repeated, free Lorentz drag at periapsis brings apoapsis to elliptical orbit at 1:1 resonance with Dione. After multiple flybys, repeated operation reaches 1:2 resonance with Enceladus, for flybys.

## 1. Introduction

Search for habitability in moons of *Outer* planets, requires presence of sources of energy. Dissipation from tidal forces is a major energy source in evolution of *Icy moon* systems. Heating always accompanies dissipation but, in case of tidal heating, it will additionally present complex spatial distribution, reflecting on a multi-layer structure in the particular case of *Icy moons*. Subsurface oceans are a generic feature of large icy bodies at some point in their evolution. A standard interior model for Icy moons consists of an outer solid (ice) layer, an intermediate liquid layer, and a solid (rocky) core.

As a satellite rises a tide on its planet, they exchange angular momentum, affecting satellite orbit and planet spin; the moon gains orbital energy at the expense of the planet rotational energy. A complex 3-body paradigm, *Laplace* resonance, involves two (or more) moons of a planet, forming by differential expansions of orbits by tidal torques. At Jupiter, moons Io, Europa, and Ganymede are in 1:2:4 resonance.

Two moons of Saturn, *Enceladus* and *Dione*, are in a 1:2 resonance: Enceladus revolution and rotation periods are both 1.370 days, Dione´s periods being approximately 2.74 days. It had been recently discovered that Enceladus ejects plumes of water vapour and ice particles, evidence of a liquid water reservoir below the surface, in the *South Polar Terrain*. More recently, in the Spring of 2017, it was found that such plumes contain molecular hydrogen, considered sign of chemical reactions supporting microbian life [1]. Very recently, in the Fall of 2018, it was brought to light a feature observed at Dione, the 4$^{4th}$ largest Saturn moon: it exhibits multiple color lines (*linear virgae*), like hundred kilometres long, parallel to the equator as latitudinal lines in a map [2]. It was suggested that such linear virgae are possibly due to impacts from dust-sized *foreign* material, with low mass and velocity to form streaks, while depositing onto the surface rather than forming craters.

After capture by a planet, here *Saturn* [3], a second stage would involve *apoapsis* lowering, to allow frequent flyby-visits to selected moons. Tether maneuvering is particular in that closed orbits after capture could *freely* evolve under repeated *Lorentz* drag. Because drag operates near periapsis, affecting it little at capture and following tether maneuvering, as later discussed, operation is comparable to capture as regards tether performance, with cathodic-contact off during flybys.

A minor tether mission could allow exploring this Laplace resonance, as it was suggested in the past to explore Jovian moons [4]. Following capture by Saturn, repeated Lorentz force around periapsis may bring the apoapsis first to an elliptical orbit at 1:1 resonance with Dione. After a number of flybys, with its *Hollow Cathode* off to explore

DOI: 10.13009/EUCASS2019-81



Dione, (as had been suggested for a minor tether mission to moon Europa [5]) repeated tether operation might bring the apoapsis down to reach a resonance with Enceladus, for further flybys.

In the present work, Sec. 2 recalls recent work on tether capture at Saturn [3], in particular showing how higher efficiency required retrograde SC orbiting, and how moon tour might, however, benefit from prograde capture. In Sec. 3 it was actually found that tangential, conveniently slow flybys of moon Enceladus, in a 1:2 resonance, are possible. Section 4 shows that Lorentz-drag peak around periapsis, greatly simplifies the analysis, and tether operation in touring Enceladus and Dione is explicitly determined. Results are discussed and conclusions summarized in Sec. 5.

## 2. Saturn *versus* Neptune Capture Review

Tether efficiency in spacecraft-capture (*S/C-to-tether mass ratio*, $M_{SC}/m_t$) goes down as $B^2$ for weak magnetic fields: The S/C relative velocity $\boldsymbol{v}' \equiv \boldsymbol{v} - \boldsymbol{v}_{\mathbf{pl}}$ induces in the magnetized ambient plasma co-rotating with the planetary spin $\Omega$, a *motional* electric field

$$\boldsymbol{E_m} \equiv \boldsymbol{v}' \wedge \boldsymbol{B} \qquad (1)$$

*in the S/C reference frame*, and $\boldsymbol{B}$ exerts *Lorentz* force per unit length

$$\boldsymbol{I} \wedge \boldsymbol{B} \qquad (2)$$

on tether current $\boldsymbol{I}$ driven by $\boldsymbol{E_m}$. Planetary capture is more effective the lower the incoming S/C periapsis because the planetary *dipole*-field **B** decreases as inverse cube of distance to the planet, so Lorentz drag decreases rapidly, as the inverse 6th power.

Also, since Lorentz-drag will peak at periapsis of a SC orbiting a planet, it will have little effect on periapsis itself. In the 2-body general relation between specific energy $\varepsilon$ and eccentricity $e$ at constant periapsis $r_p$,

$$\varepsilon = (e - 1)\, \mu/2r_p, \qquad (3)$$

any sequence of drag-work steps will directly relate $e$ and $\varepsilon$. For a SC *Hohmann*-transfer between heliocentric circular orbits at Earth and planet, the arriving velocity $v_\infty$ of the hyperbolic orbit in the planetary frame provides an orbital specific energy

$$\varepsilon_h = \tfrac{1}{2}\, v_\infty^{\,2}.$$

Using $v_\infty$ in (3) yields

$$e_h - 1 = v_\infty^2\, R / \mu \qquad (4)$$

where $\mu$ is the gravitational constant and we took periapsis $r_p \approx R$. A Jovian gravity-assist [6] can reduce $v_\infty$, and thus eccentricity, helping magnetic capture of a SC into elliptical orbit.

Planetary capture, requiring negative Lorentz drag-work, $W_d/M_{SC} = \Delta\varepsilon < 0$, allows writing

$$\frac{|W_d|}{m_t} = \frac{|W_d|}{M_{SC}} \times \frac{M_{SC}}{m_t} = \left|\Delta\varepsilon\right| \times \frac{M_{SC}}{m_t} \qquad (5)$$

We will find $\left|W_d\right| / m_t$ to be a function of just ambient conditions. Greater capture efficiency in (5) thus requiring lower $\left|\Delta\varepsilon\right|$, an optimum value corresponds to eccentricity after capture $e_c$ being just below unity. This allows to calculate efficiency from drag work along the parabolic orbit at periapsis. Using (3) and (4), we finally find an expression for capture efficiency, depending on Lorentz drag work and the hyperbolic velocity $v_\infty$,

$$\frac{|W_d|}{m_t v_\infty^2/2} = \frac{M_{SC}}{m_t} \times \frac{e_h - e_c}{e_h - 1} \sim \frac{M_{SC}}{m_t}$$

We calculate drag work

$$\dot{W}_d = \bar{v} \bullet \left[ L_t\, \bar{I}_{av} \wedge \bar{B} \right] = -L_t\, \bar{I}_{av} \bullet \left( \bar{v} \wedge \bar{B} \right) \qquad (6)$$

DOI: 10.13009/EUCASS2019-81



using length-averaged current $I_{av}$ as bounded by the *short-circuit* value, $\sigma_t E_m \times h_t w_t$, with $\sigma_t$, $h_t$ and $w_t$ being tape-tether conductivity, thickness and width,

$$L_t \bar{I}_{av} = L_t \times i_{av} w_t h_t \sigma_t E_m \times \bar{u}_I , \qquad i_{av}(L_t / L_*) < 1 \qquad (7)$$

$L_*$ being certain characteristic ambient-plasma length $\propto (E_m/\mathrm{N_e}^2)^{1/3}$ [7], and $I_{av}$ only depending on electron density through $i_{av}$. With tether along the motional field $\boldsymbol{E_m}$, power in Eq.(6) becomes, using Eq.(1),

$$\Rightarrow \qquad \dot{W}_d = -i_{av}\sigma_t L_t w_t h_t \times \left(\bar{v}' \wedge \bar{B}\right) \bullet \left(\bar{v} \wedge \bar{B}\right) = -i_{av}\sigma_t \frac{m_t}{\rho_t} B^2 \bar{v}' \bullet \bar{v} \qquad (8)$$

From conservation of angular momentum we find

$$\bar{v} \bullet \bar{v}' = \bar{v} \bullet \left(\bar{v} - \Omega r \bar{u}_\theta\right) = v^2 - \Omega r v_\theta = v^2 - \Omega r_p v_p \qquad (9)$$

Using here, explicitly, $v^2 = 2\mu / r$ from the energy equation for parabolic orbits, there immediately results

$$\bar{v} \bullet \bar{v}' = v^2 \left(1 - r \frac{\Omega r_p v_p}{2\mu}\right) = v^2 \left(1 - \frac{r}{r_M}\right) \qquad (10)$$

$$r_M / r_p \equiv \sqrt{2} \times \left(a_s / r_p\right)^{3/2} \propto \left(\rho_{pl} / \Omega^2\right)^{1/2} \qquad (11)$$

with $r_M$, where $\bar{v} \bullet \bar{v}'$ changes sign, being the maximum radius presenting drag, and $a_s = (\mu / \Omega^2)^{1/3}$ being the radius of an equatorial circular orbit, where velocities of SC and co-rotating plasma are equal, $(\mu / a_s)^{1/2} = \Omega a_s$. The last expression in (11) applies in the present analysis, where $r_p \approx R$.

We shall use values at $a_s$ as reference values, introducing the magnetic dipole law to write $B(r) = B_s a_s^3 / r^3$. Next, using (10) in Eq.(8), and the radial speed rate in parabolic orbits, we can now determine drag work

$$\int_{\Delta t} \left|\dot{W}_{d1}\right| dt = 2 \times \int_R^{r_M} \frac{\dot{W}_{d1} dr}{dr/dt}, \qquad \frac{dr}{dt} = \frac{\sqrt{2\mu\left(r - r_p\right)}}{r} \qquad (12a, b)$$

finally yielding,

$$\left|W_{d1}\right| / \frac{1}{2} m_t v_\infty^2 \equiv \tilde{B}_s^2 \times \tilde{W}_1 \qquad \tilde{B}_S^2 = \sigma_t B_S^2 a_s v_s / 2^{5/6} \rho_t v_\infty^2 \qquad (13a, b)$$

$$\tilde{W}_1 = 2 < i_{av} >_r \times \tilde{r}_M^{\,8/3} \int_1^{\tilde{r}_M} \frac{d\tilde{r}}{\tilde{r}^6 \sqrt{\tilde{r} - 1}} \left(\tilde{r}_M - \tilde{r}\right), \qquad (\tilde{r} \equiv r / r_p) \qquad (14)$$

where we use subscript 1 to later recall that Eq. (14) applies to value $e = 1$. As regards the above radial-average of the normalized length-average current $\mathrm{i_{av}}$, consider the particularly simple regime for $L_t / L_* > 4$

$$1 - i_{av} = \frac{L_*}{L_t} \left[\propto \frac{E_m^{1/3}}{L_t} \times \left(\frac{\sigma_t h_t}{N_e}\right)^{2/3}\right], \qquad \frac{L_*}{L_t} < \frac{1}{4} \qquad (15)$$

yielding $i_{av} > 0.75$ [7]. If this regime applies at the lowest relevant $N_e$ values, it should allow writing $< i_{av} >_\mathrm{r} \approx 1$. However small plasma density $N_e$ might reasonably be, it may be balanced by using a long enough tether. Note that this would favour using tethers for heavier SC. Actually, a longer tether may keep the same mass by reducing width, condition for validity of the standard OML (*orbital motion limited*) regime on current collection by a tether, is keeping $w_t$ <u>below</u> some upper bound, roughly 4 *times Plasma Debye length*.

Note now the very steep decrease away from periapsis in the radial rate of (14), as advanced,

$$1 / \tilde{r}^6 \sqrt{\tilde{r} - 1} \qquad (16)$$

Calculations of the integral not requiring to go far from $\tilde{r} = 1$. Independently, $r_M$ places a definite limit to the range of integration. Which limitation is more effective, depends on the $r_M$ value. For a large value, case of Neptune, as shown in Table.1, one can just ignore $r$ in the numerator inside the integral, altogether.

DOI: 10.13009/EUCASS2019-81



On the other hand, for a smaller $r_M$ as in the case of Saturn, it pays to eliminate its limiting character by moving from *prograde* to retrograde orbiting, just writing $r_M + r$ in that numerator, with a gain in the integral (and in capture efficiency) of about 2. The integral converges very rapidly, increasing from 0.971 $\tilde{r}_M$ to just 1.008 $\tilde{r}_M$, if taking the upper limit from 1.5 to 2 [3]. In the present work we will go back to prograde capture, the drop by half in capture efficiency not being determinant here. Our goal is allowing slow flybys exploration of the moons concerned.

| | Saturn | Neptune |
|---|---|---|
| $\rho_{pl}$ (gr/cm$^3$) | 0.6871 | 1.638 |
| Period (hours) | 10.656 | 16.11 |
| Drag reach $r_M$ (in parabolic orbit) | $3.7 R_S$ | $8.9 R_N$ |
| Dipole Tilt | $< 0.5°$ | 47° |
| Dipole Offset ($f R$) | $0.06 R_S$ | $0.55 R_N$ |

**Table 1 Saturn/Neptune Comparison**

Table 1 clearly shows that Saturn and Neptune present opposite cases among the Outer Giant Planets as regards density and spin, as emerging from the last expression in (11), resulting in opposite extremes in radial reach of Lorentz drag, $3.7R_S$ as against $8.9R_N$. Another basic difference among Outer Giants arises from the magnetic structure of the field B. A planetary magnetic field is due to a system of stationary currents in small volumes inside, as described by its magnetic moment and dipole law.

The Saturn dipole is located at its center and is parallel to the rotation axis; this holds approximately for Jupiter, too. On the other hand, the Neptune dipole is highly tilted and offset. For Neptune capture, efficiency depends on the longitude at periapsis; Fig. 1 shows the optimum case, with the SC facing the dipole when reaching periapsis, with minimum distance to the dipole, $\rho$. Lorentz drag decreasing with the inverse 6th power of $\rho$, faster convergence in the capture work integral allows not to go beyond about 1.12 $r_p$, as against 1.5 $r_p$ for Saturn. Both basic differences between extreme Saturn and Neptune cases, suggest that joint missions to different planetary systems of moons might not be effective.

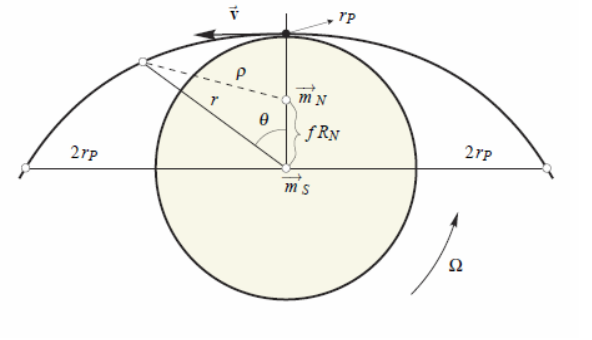


**Figure 1 Position of the magnetic dipole and approximate S/C trajectory**

There is a further condition that separates Neptune of the other 3 Outer Giants. It has just 1 large moon, Triton, which is in retrograde orbit. Although unnecessary for greater capture efficiency because of the large 8.9 $R_N$ value, visiting that moon will certainly need retrograde capture. Along with the final Outer planet, Uranus, having its rotation axis nearly lying in the ecliptic plane, both singular differences might be signs of collisions with other big bodies in the intriguing, early Solar System dynamics.

## 3. Moon / Spacecraft resonances

Following capture, the SC apoapsis can be lowered, at given periapsis, to a circular moon orbit, allowing for a 1:2 resonance with the SC elliptical orbit if the moon orbital radius satisfies certain condition. This would allow conveniently slow, tangential SC flybys of the moon; with two periapsis passes for each flyby. In the present problem the periapsis value was fixed, $r_p \approx R_S$, to make capture efficient, as we argued at length above. We have just found that moon Enceladus does satisfy the condition for that 1:2 resonance:

The period of a moon circular orbit of radius $r_m$, around a planet with gravitational constant $\mu$, is $\tau_m = 2\pi\, r_m^{\,3/2} / \sqrt{\mu}$. The period of an elliptical orbit with given periapsis $r_p$, and apoapsis at $r_m$, *eccentricity* being $e_{SC} = (r_m - r_p) / (r_m + r_p)$, is

$$\tau_{SC} = \frac{2\pi}{\sqrt{\mu}}\left(\frac{r_p}{1-e_{SC}}\right)^{3/2} = \frac{2\pi}{\sqrt{\mu}}\left(\frac{r_m}{1+e_{SC}}\right)^{3/2} \qquad (17)$$

Condition for a 1:2 resonance being $\tau_m = 2\tau_{SC}$, there results $(1 + e_{SC})^{3/2} = 2$, i.e.

$$\left(\frac{2r_m}{r_m + r_p}\right)^{3/2} = 2 \quad \Rightarrow \quad \frac{r_m + r_p}{r_m} = 1.2534 \approx 2^{1/3} = 1.2599 \qquad (18)$$

where we used values $r_p \approx R_S \approx 60300$ km and $r_m = r_{Enc} \approx 238000$ km. There is fair agreement with the condition of moon-spacecraft 1:2 resonance at Enceladus.

DOI: 10.13009/EUCASS2019-81



Certainly, the 1:2 resonance does not apply to moon Dione, for which we will use non-tangential flybys at 1:1 resonance, with one periapsis pass per flyby. Now we will have $\tau_{SC} = \tau_D$, i.e.,

$$\frac{2\pi}{\sqrt{\mu}}\left(\frac{r_p}{1-e_{SC}}\right)^{3/2} = \frac{2\pi}{\sqrt{\mu}} r_D^{\,3/2} \qquad (19)$$

yielding $1 - e_{SC} = r_p / r_D \approx 0.160$, having used $r_D \approx 377400$ km and $r_p \approx R_S$. We thus find $e_{SC} \approx 0.840$, with the apoapsis of the orbit at 1:1 resonance with *Dione*, $r_a = (1 + e_{SC}) \times r_D \approx 694400$ km, lying between moons *Rhea* and *Titan.* Note that 1 revolution period of moon Dione (2.74 days) does correspond to 1 periapsis pass of the SC during Dione flybys, whereas it corresponds to 4 SC periapsis passes (0.685 days) during the Enceladus flybys, when Dione, Enceladus, and the spacecraft are in 1:2:4 resonance.

Apoapsis lowering will occur at successive periapsis passes, resulting in a series of elliptical orbits with common periapsis and decreasing eccentricities, with changes in periapsis position being small second-order effects. As noticed in the following section, Eccentricity decrements being small, about 0.02 say, like at capture itself calculations may be carried out as if eccentricity, though different from unity, was kept constant during each perijove pass. Changes in calculation, as compared with the capture analysis, are using the energy equation for each particular eccentricity value,

$$v^2 = \mu\left(\frac{2}{r} - \frac{1-e}{r_p}\right) \qquad (20)$$

instead of $v^2 = 2\mu / r$, while, instead of Eq.(12b), using the radial speed rate $dr/dt$ value resulting from (20) and the angular-momentum conservation law,

$$r^2 d\theta / dt = r_p v_{pe} \qquad (21)$$

We then have

$$\left(\frac{dr}{dt}\right)^2 = v^2 - \left(r\frac{d\theta}{dt}\right)^2 = \mu\left(\frac{2}{r} - \frac{1-e}{r_p}\right) - \frac{(1+e)\mu r_p}{r^2} \qquad (22)$$

where we used the periapsis velocity $v_{pe} = [\mu(1+e)/r_p]^{1/2}$. Radial speed-rate vanishing, in (22) above, occurs at 2 values of radius, periapsis $r_p$ and apoapsis $r_a = r_p(1+e)/(1-e)$, finally yielding

$$\frac{dr}{dt} = \sqrt{(1+e)\mu(r-r_p)[1-(r/r_a)]}\,/\,r \qquad (23)$$

replacing Eq.(12b) for $e = 1$, when the apoapsis radius $r_a = r_p(1+e)/(1-e)$ lies at infinity.

Next, use (20) in Eq.(9), and write

$$r\bar{v}\bullet\bar{v}' = r\left[\mu\left(\frac{2}{r} - \frac{1-e}{r_p}\right)\right] - r\Omega r_p v_{pe} = 2\mu\left[1 - \frac{r}{r_p}\frac{1-e}{2} - r\frac{\Omega r_p}{2\mu}\sqrt{\frac{\mu(1+e)}{r_p}}\right]$$

$$\Rightarrow \quad r\bar{v}\bullet\bar{v}' = 2\mu\left[1 - \tilde{r}\,\frac{1-e}{2} - r\frac{\Omega r_p}{2\mu}\sqrt{\frac{\mu(1+e)}{r_p}}\right] = 2\mu\left[1 - r\left(\frac{1-e}{2r_p} + \sqrt{\frac{1+e}{2}}\,\frac{1}{r_M}\right)\right] \qquad (24)$$

replacing $2\mu\left[1-(r/r_M)\right]$, from Eq.(10), for $e = 1$.

DOI: 10.13009/EUCASS2019-81



## 4. A Dione-Enceladus tour scheme

Using Eqs. (23) and (24) as the indicated replacements in Eq. (13a) yields

$$\frac{|W_{de}|}{m_t v_\infty^2/2} = \tilde{B}_s^2 \tilde{W}_e, \qquad \tilde{B}_s^2 = \frac{\sigma_t B_s^2 a_s v_s}{2^{5/6} \rho_t v_\infty^2} \qquad (25a,b)$$

$$\tilde{W}_e \equiv 2 < i_{av} >_r \tilde{r}_M^{8/3} \int_1^{\tilde{r}_u} \frac{d\tilde{r}}{\tilde{r}^6 \sqrt{\tilde{r}-1}} \times \frac{\tilde{r}_M - \tilde{r}\left[\sqrt{(1+e)/2} + \tilde{r}_M (1-e)/2\right]}{\sqrt{\left[(1+e) - (1-e)\tilde{r}\right]/2}} \qquad (26)$$

where Eq. (25a) replaces (13a), Eq. (25b) is just Eq.(13b), and $\tilde{r}_M$ keeps being 3.7. Note that Eq. (26) does indeed recover Eq.(14) for $e \to 1$.

As $e$ is decreased from 1, the upper limit in the integral keeps being the $r$-value for vanishing numerator in the second ratio above, until a value $e \approx 0.28$ is reached with denominator vanishing too. At lower $e$, the upper limit in the integral is the apoapsis radius, at vanishing denominator. Note that this change in behavior occurs well below the $0.84 < e < 1$ range involved in reaching resonance with Dione and its flybys exploration, and below the $0.60 < e < 0.84$ range required for the Enceladus flybys.

An approximate, extremely simplified analysis is here discussed. For the eccentricity ranges of interest, $0.84 < e < 1$ and $0.60 < e < 0.84$, and $1 < r/r_p < 1.5$, the last ratio in (26) may be reasonably approximated as $(r_M - r)/r_p$, with Eq (26) then replaced by (14). For $r = r_p$ and $e = 0.84$ and 0.60, that ratio yields 2.66 and 2.67 respectively, whereas $(r_M - r)/r_p = 2.70$ independently of eccentricity, with respective errors -1.5% and -1.1%. For $r = 1.5 r_p$ and $e = 0.84$ and 0.60, that ratio yields 2.03 and 1.78 respectively, whereas $(r_M - r)/r_p = 2.2$ independently of eccentricity, with respective errors – 7.5% and -- 19%. The error is now substantial, particularly at the lower eccentricity. Let us recall, however, the very steep decrease away from periapsis, in the radial rate, given in (16), at both Eqs. (14) and (26), making values around $r = 1.5\, r_p$ contribute negligibly to integrals involving that rate, as noticed in the paragraph following Eq. (16). Results from the simplified analysis would reasonably apply for the $0.60 < e < 1$ tour.

### 4.1 *Moon tour*

With Eq. (14) replacing (26) in the above simplified analysis, SC-orbit evolution can be described in terms of number of successive periapsis passes. For $M_{SC}/m_t$ such that $e_c$ is about 0.99, it would take 7 steps following capture, for the SC to reach $e = 0.85$, with the capture value $\Delta e \approx 0.02$. A last eccentricity decrement must be reached in two convenient steps by switching the current off appropriately over part of the drag arc to allow for a first flyby of Dione while reducing $\Delta e$ by half. Switching off the current afterward over the entire resonance orbit would allow for repeated flybys, with the moon overtaking each time the SC. It would take 12 steps to reach Enceladus at e = 0.60 from Dione at $e = 0.84$.

### 4.2 *Power generation*

A very large amount of energy could be taken from the orbital motion of the SC during capture and during each one of the successive periapsis passes, into the tether electric circuit. A fraction taken by electric loads at the cathodic end, could have a weak effect on tether current, and the related tether dynamics. A part of that energy could be used during each of the operation steps, with the rest saved/stored in batteries, for later use. Operation would keep emphasis on reserving power for use at the planned steps at Enceladus, main objective of the mission, as regards life search.

The revolution period of Dione is about 2.74 days. The SC at resonance 1:1 would take 13.70 days in making 5 flybys. The SC at resonance 1:2 would take 1 flyby per period of Enceladus, or 13.70 days in making 10 flybys.

### 4.3 *Minor issues*

Radiation is a big issue for tethers at Jupiter but not at Saturn, which lacks strong radiation belts. As regards tether dynamic instabilities, they are generally quite slow [8], while the times involved in the mission are short. Regarding the $J_2$ zonal harmonic coefficient, which is 15 times as large as Earth's, and comparable to Jupiter, it requires a minor correction involving apsidal precession, the way it was made for Jupiter, to consider in planning an Enceladus-Dione mission.

DOI: 10.13009/EUCASS2019-81



## 5. Summary of results

Saturn moon *Enceladus* stands out, along with Jovian moon *Europa*, as particular *object of interest* in the search for conditions of habitability, in parallel to search for life, in the *ice moons* of the *Outer Giant Planets.* Moons Enceladus and *Dione* are in 1:2 resonance in the Saturn system. The very recent discovery (fall of 2018), as result of mission Cassini, of intriguing *linear virgae* at *Dione*, makes exploring both moons a necessity. We have presented a tether-mission concept making possible multiple flybys of both moons, though Enceladus would be of most critical interest. We have proved that a SC orbit at Saturn with periapsis very near planet radius and apoapsis at Enceladus orbit satisfies the condition for a 1:2 moon/SC resonance, allowing conveniently slow parallel SC flybys of the moon. Our analysis shows that following magnetic capture by the SC-tether, repeated free Lorentz-drag, keeping periapsis near constant, could take the SC apoapsis down to Enceladus.

## Acknowledgements

This work was supported by MINECO/AEI, under Project ESP2017-87271-P, and under FEDER/EU

## References

[1] Waite, J. H. *et al*. 2017. Cassini finds molecular hydrogen in the Enceladus plume: Evidence for hydrothermal processes. *Science* 356: 155-159.

[2] Martin, E. and A. Patthoff. 2018. Mysterious Linear Features across Saturn's Moon Dione. *Geophys. Res. Letters* 45: 10027-30.

[3] Sanmartin, J. R., J. Pelaez, and I. Carrera-Calvo. 2018. Comparative *Saturn-versus-Jupiter* Tether Operation. *J. Geophys. Res.: Space Physics* 123:6026-030.

[4] Sanmartin, J. R. *et al*. 2009. Electrodynamic Tether at Jupiter – II: Fast Moon Tour after Capture. *IEEE Trans. Plasma Sci.* 37:620-626.

[5] Sanmartin, J. R., M. Charro, H. B. Garrett, G. Sánchez-Arriaga, and A. Sánchez. 2017. Analysis of tether-mission concept for multiple flybys of moon Europa. *J. Prop. Power* 33: 338.342.

*[6]* Battin, R.H. 1999. An introduction to the mathematics and methods of astrodynamics. AIAA education series.

[7] Sanmartin, J. R. *et al*. 2008. Electrodynamic Tether at Jupiter – I: Capture Operation and Constraints. *IEEE Trans. Plasma Sci.* 36:2450-2458.

[8] Peláez, J., E. C. Lorenzini, O. López-Rebollal, and M. Ruiz. 2000. A New Kind of Dynamic Instability in Electrodynamic Tethers. *J. Astronautical Sciences* 48: 449-476.